Anatomical and Histological Analysis of a Complex Structure Too Long Considered a Simple Ligament: The Filum Terminale

Thiébaud Picart, Marc Barritault, Emile Simon, Philip Robinson, Cédric Barrey, David Meyronet, Patrick Mertens

Version of Record: https://www.sciencedirect.com/science/article/pii/S1878875019314615
Manuscript_aa3a6cbc132aff52b5802b5f8fd2753f

Anatomical and histological analysis of a complex structure too long considered as a simple ligament: the *Filum Terminale*

Thiébaud Picart[a]

Marc Barritault[b,c]

Emile Simon[a,d]

Philip Robinson[e]

Cécric Barrey[a]

David Meyronet[c,f]

Patrick Mertens[a,c,d]

a. Hospices Civils de Lyon
Hôpital Neurologique Pierre Wertheimer
Department of Neurosurgery
59 boulevard Pinel
69667 BRON, France

b. Hospices Civils de Lyon
Groupe Hospitalier Est
Department of Molecular Biology
59 Boulevard Pinel
69394 BRON, France

c. Claude Bernard Lyon 1 University
Faculty of Medicine Lyon Est
69373 LYON CEDEX 08, France

d. Laboratory of Anatomy
Faculty of Medicine Lyon Est
University Claude Bernard Lyon 1
69373 LYON CEDEX 08, France

e. Hospices Civils de Lyon
Direction de la Recherche Clinique et de l'Innovation
47 rue Villon

69008 LYON

f. Hospices Civils de Lyon
Groupe Hospitalier Est
Department of Neuropathology
59 Boulevard Pinel
69394 BRON, France

Thiébaud Picart, MD, MSc – thiebaud.picart@chu-lyon.fr

Marc Barritault, MD, PhD – marc.barritault@chu-lyon.fr

Emile Simon, MD, PhD – emile.simon@chu-lyon.fr

Philip Robinson, PhD – philip.robinson@chu-lyon.fr

Cécric Barrey, MD, PhD – cedric.barrey@chu-lyon.fr

David Meyronet, MD, PhD – david.meyronet@chu-lyon.fr

Patrick Mertens, MD, PhD – patrick.mertens@chu-lyon.fr

Corresponding author:

Dr Thiébaud PICART

Department of Neurosurgery

Hôpital Neurologique Pierre Wertheimer

59 boulevard Pinel

69667 BRON

France

Tel +33689621871

Fax +33472357847

thiebaud.picart@chu-lyon.fr

Keywords: Anatomy; Ependymoma; Filum Terminale; Histology; Spine; Tethered Cord Syndrom

Running title: Filum Terminale: anatomical and histological study

Anatomical and histological analysis of a complex structure too long considered as a simple ligament: the *Filum Terminale*

Abstract

Background: The intradural *Filum Terminale* (iFT) connects the *Conus Medullaris* (CM) with the Dural Sac (DS) and the extradural *Filum Terminale* (eFT) connects the DS to the coccyx. The aim is herein to update the description of the FT and to integrate these data in a physiopathological context.

Methods: Anatomical measurements and histological investigation were performed on ten human cadavers.

Results: The mean lengths of the iFT and eFT were 167.13 and 87.59 millimeters, respectively. The mean cranial diameter of the iFT was 1.84 millimeter. It exceeded 2 millimeters in two specimens. The mean half and caudal diameters of the iFT were 0.71 and 0.74 millimeter, respectively. The cranial diameter of the eFT was correlated with the caudal diameter of the eFT (ρ=0.94, p=.02). The level of CM-iFT junction was significantly correlated with the iFT length (ρ=-0.67, p=.03). The mobilization of the iFT was not transmitted to the extra-dural elements and *vice-versa*. The iFT contained axons and ependymal cells which were dense in the first third and then caudally randomly arranged in islets. This could explain why ependymomas can occur all along the iFT. Ganglion cells were abundant around the junction with the DS. The eFT contained smooth muscle cells, adipocytes and axons. A mechanoreceptor was identified in one specimen.

Conclusions: Consistently with their common embryological origin, there is a real anatomical and histological continuum between the CM and the FT. The FT should therefore no longer be considered as a simple ligament but rather as a complex fibro-cellular structure.

Acknowledgements: We warmly thank Mrs. Tilia Mézières and Mrs. Vanessa Nirdé for their precious technical assistance.

Funding sources: none

Conflict of interest: None

INTRODUCTION

The development of the *Filum Terminale* (*FT)* results from the dedifferentiation of the caudal part of the embryonic and fetal Spinal Cord (SC).[1–4] After birth, the FT connects the *Conus Medullaris* (CM) and the coccygeal periosteum.[5] More precisely, the intradural FT (iFT) is the cranial portion of the FT that lies between the CM and the DS, while the extradural FT (eFT = *Ligamentum Coccygeale*), constitutes the caudal portion of the FT, thus linking the Dural Sac (DS) and the coccyx.[2,6–8] The anatomical studies dedicated to the FT are relatively scarce and most are not recent.[6,8–15] Histologically, the adult FT has long been considered as a fibrous structure and the identification of cellular elements in its vicinity is recent.[2,7] Obviously, malformations or tumors of the FT are likely to generate neurological disorders because of its close relationship with the SC and the *Cauda Equina* (CE).[5] The aim of the present study was therefore to update the anatomical and histological description of the FT, and to integrate these data in a physiopathological context.

MATERIAL AND METHODS

Ten human cadavers from adults who donated their bodies to science for anatomical purposes were included. For each specimen, demographic characteristics and morphometric parameters were collected. As summarized in Table 1, 50% of specimens were women and 50% were men. With the exception of degenerative scoliosis in one specimen, no obvious neural or orthopedic abnormality was noted.

Dissection protocol

After prone positioning, a midline dorsal longitudinal skin and aponeurotic incision was performed from the ninth thoracic vertebra to the coccyx. After dissection of the subcutaneous and muscular plans, spinous processes and laminae from the tenth thoracic vertebra to the fifth sacral vertebra and the coccyx were exposed. A laminectomy was performed from the tenth thoracic vertebra cranially to the sacral hiatus caudally in order to expose the DS, the emerging nervous roots, and the eFT. After careful longitudinal opening of the DS from the tenth thoracic vertebra to its termination, the CM, the CM-iFT junction, the iFT and the CE were exposed. By convention, the end of the CM was defined as the level of emergence of the last coccygeal roots[5,7].

Anatomical study

The shape of the FT, its relationships with the arachnoid and the CE were thoroughly examined. Then, the FT was carefully removed "en bloc" with a collar of dura-matter to preserve the FT-DS junction. Caudally, a fragment of coccygeal periosteum was detached to guarantee the integrity of the eFT. The levels of the CM-iFT junction, FT-DS junction, and the insertion of the FT on the coccygeal periosteum were noted thanks to benchmarks precisely set before the removal of the FT. As previously proposed[2,6,8,11,14,15], each vertebra was divided into thirds to increase the precision of the description. The lengths of the iFT and eFT, the diameters of the iFT at different points (origin, first quarter, half, third quarter, and termination), and the diameters of the eFT (origin, half, and termination) were determined with a digital Vernier caliper.

Histological study

The specimens were fixed in zinc formalin. After paraffin embedding, longitudinal 4µm-thick sections were made. Sections were stained with hemalum-phloxine-saffron to highlight cellular and fibrous elements. Complementary staining using luxol-fast-blue, neurofilament, NeuN, and actin were performed to highlight myelinated structures, neural structures, Ganglion Cells (GC) and Smooth Muscular Cells (SMC), respectively.

Statistical analysis

A statistical analysis was performed using R software (R foundation for Statistical Computing, Vienna, Austria, version3.5.1) to investigate correlations using the Pearson correlation coefficient and the Spearman correlation coefficient for quantitative and ordinal variables, respectively. The level of significance was set at 5% ($p<.05$).

RESULTS

Microsurgical anatomy

The iFT was easily differentiated from the CE roots (CEr) thanks to its characteristic pearly white color. Conversely, the eFT did not always have the same hue and could also appear greyish or translucent.

1. iFT

As the very proximal portion of the iFT was anterior to the lumbar and sacro-coccygeal roots, the CM-iFT transition was not directly seen after opening the dura mater (Figure 1A). The exposure of the CM-iFT transition revealed the progressive appearance of fibrous tissue organized in linear spans within the CM. In parallel, the nervous tissue became less abundant and disappeared completely about 1 millimeter below the emergence of the last coccygeal roots. At this level, the fibrous spans converged towards a common origin which should be considered as the starting point of the FT (Figure 1B).

The iFT had a close relationship with the CEr and its relative position compared to the roots changed gradually during its intradural course. Its central and distal parts were clearly posterior to the roots. Adhesion of nervous rootlets to the iFT were observed. They were located in the proximal portion of the iFT in three cases (30%) and in the most distal portion of the iFT in five cases (50%). In two cases (20%), a rootlet was intertwined with the FTi.

Only the posterior surface of the iFT was in contact with the arachnoid membrane. The contact was direct in three cases (30%) while a film of cerebrospinal fluid was interposed between these two structures in the remaining cases (70%). The iFT was in the same sub-arachnoidal compartment as the CEr except in one specimen in which there was a longitudinal septum isolating the iFT and some CEr from the remaining roots. The iFT was either hourglass shaped (70%) or cone-shaped (30%).

2. FT-DS junction

There was a *continuum* between the FT and the DS (Figure 1C). This fusion area was most frequently centered on the median line (80%) and sometimes lateralized on the right (10%) or left (10%)

3. eFT

The eFT lay against the posterior vertebral wall, anteriorly to the CE, in an adipose environment until it came out of the sacral channel through the sacral hiatus. Its path continued either in contact with the coccygeal periosteum or with the posterior sacro-coccygeal ligament. The eFT was free of any attachment, except in its last centimeter where osteo-periosteal attachments were inconstantly found.

The periosteal insertion of the eFT was located on the posterior surface of the coccyx and was polymorphic. In its most common form, it was Y-shaped and located on the midline (50%) or lateralized on the right (10%). In the remaining cases, there were either a single bundle inserted in a punctual zone (20%, Figure 1D) or several bundles (at least three) that were fan-shaped (20%, Figure 1E). The shape of the eFT was more constant since 9 eFTs (90%) were cone-shaped and one (10%) hourglass-shaped.

4. Vascular elements

Proximally, the arterial vasculature of the FT was provided by a small artery that was connected to the anterior spinal artery. A bifurcation was sometimes noticed at the proximal part of the iFT but, in this case, one of the two branches was dominant. Distally, the artery of the iFT was connected with several vessels distributed in the iFT.

A vein of variable caliber, often thin (80%) but appearing dilated in two specimens (20%), was found posteriorly to the iFT artery. Insofar as this vein had no collateral branches, it seemed improbable that it could provide the venous drainage of the iFT.

Morphometric parameters

As summarized in Table 2, the mean lengths of the iFT and eFT were 167.13 millimeters and 87.59 millimeters, respectively. The mean diameter of the iFT ranged from 1.84 millimeter at its origin to 0.74 millimeter at its termination with an intermediate shrinkage. In 2 specimens, the initial diameter of the iFT excessed 2 millimeters and in one of them, the CM was in a low position (L2L3 disc). The mean diameter of the eFT decreased progressively from 1.05 millimeter to 0.59 millimeter, consistently with the predominant cone-shape.

The distribution of the CM-iFT junction was Gaussian, centered on the L1L2 in female specimens and more variable in male specimens. The levels of the iFT-DS-eFT and

eFT-coccyx junctions were more constant and centered on the lower third of S2 (60% of cases) and the second coccygeal vertebra (80% of cases), respectively (Figure 2).

There was no significant correlation between the height of the specimen and the iFT length (ρ=0.43, p=0.21) or the eFT length (ρ=0.37, p=0.29). The iFT and eFT lengths were also not correlated (ρ=0.34, p=0.32). The comparison of the different diameters of iFT and eFT with each other in all possible combinations found only one statistically significant correlation: the proximal diameter of the eFT was correlated with the distal diameter of the eFT (ρ=.94, p=0.02).

The level of CM-iFT junction was significantly correlated with the iFT length (ρ=-0.67, p=0.03) but neither with the specimen height (ρ=-0.12, p=0.73) nor the length of the eFT (ρ=0.23, p=0.51). The level of iFT-DS-eFT junction was neither correlated with the specimen height (ρ=-0.22, p=0.52), the length of the iFT (ρ=-0.22, p=0.53), the length of the eFT (ρ=-0.56, p=0.09), nor the level of CM-iFT junction (ρ=-0.06, p=0.85).

Mobilization of the FT

Although cranial and caudal tractions of the iFT resulted in concomitant mobilization of the CM and DS, respectively, the movements were neither transmitted to the eFT nor to the CEr. Reciprocally, cranial and caudal tractions of the eFT were transmitted to all the CEr in their extradural portion. Whereas very few movements were transmitted to the DS, the iFT and the CM remained static.

Histological structure

As macroscopically observed, the CM-iFT transition is progressive since there is a gradual depletion of glial and neuronal cell elements with a strong enrichment in connective tissue. Peripherally, the pia mater was thickened. At this level, included axons, myelinated or not, were found in all specimens (Figure 3A). The iFT-CM junction was also enriched in ependymal cells organized in tubes or rosettes (Figure 3B). The persistence of ependymal cells, randomly arranged in islets, beyond the first third of the iFT, was noted in five specimens (50%). NeuN-immunopositive GC were randomly distributed within the CM-iFT junction (Figure 3C and insert) and in the first half of the iFT (Figure 3D) in five specimens (50%). In nine specimens (90%), amyloid bodies were present within the cellular areas of the

proximal part of the iFT (Figure 3E). Nervous elements were abundant at the close periphery of the iFT (Figure 3F) and were sometimes myelinated, as highlighted by luxol-fast-blue staining (Figure 3G), but also within the iFT (Figure 3H, 3I).

In five specimens (50%), the iFT-DS junction was particularly enriched in GC which were anarchically disposed (Figure 3J).

In the eFT of one specimen, a structure composed of a circular cluster of neuronal cells organized in sheets was found (Figure 3K) and probably corresponded to a mechanoreceptor. The proximal eFT contained included axons (Figure 3L) and calcospherites within connective tissue areas (Figure 3M). SMC were constantly present in the whole eFT (Figure 3L and 3N) as highlighted by the immunostaining for actin (Figure 3N insert). Adipocytes were found around the eFT and within the most distal portion of the eFT (Figure 3O), as was fibrous tissue (Figure 3P).

DISCUSSION

Anatomical considerations

The definition of the iFT origin remains elusive.[5,7] *In fine*, the CM-iFT junction is not punctual but instead corresponds to a transition zone where the nervous tissue of the CM is progressively replaced by fibrous tissue spans converging at a point that seems to relevantly and objectively define the origin of the iFT.

The iFT-DS-eFT junction has been very rarely studied.[2] It has either been described as a "perforation" of the DS by the iFT[16] or as a "fusion", given the *continuum* between the FT fibrous stroma and the dura-mater.[2,6,7] The description herein is in accordance with this second term and remains consistent with the embryological data. Indeed, the FT originates from the dedifferentiated distal portion of the embryonic SC which fuses with the dura-mater that previously covered it.[1,7] In series reported herein, the iFT-DS-eFT junction was located outside the sagittal medial line in 20% of cases while it was so in 11% of cases in the study reported by Hansasuta *et al.*[6] This anatomical data must be kept in mind when looking for the iFT in its distal portion through a restricted surgical approach.

The termination of the eFT has been considered as a blend of the eFT fibers and the coccygeal periosteum.[7] The polymorphism of this termination with one or several bundles described in the present study is original.

Analysis of morphological and biomechanical parameters

The mean lengths of the iFT and eFT herein are approximately 10 mm longer than the values previously published[2,7,9,10,12,17] (Table 3) probably because the specimens were not fixed with formaldehyde that is responsible for retraction and restriction of the measured lengths.[18] We confirmed the absence of correlation between the specimen height and the iFT length.[2,12,17] Conversely, the correlation between the specimen height and the eFT length previously described by De Vloo *et al.*[2], Pinto *et al.*[12] and Nasr *et al.*[17] was not found. The diameters of the iFT and the eFT are comparable to those obtained in other studies[2,9,12,17] (Table 3). However, the correlation between the 4 most caudal diameters of the iFT and between the 3 diameters of the eFT, identified by De Vloo *et al.*[2] were not validated in this series.

The median level of the CM-iFT junction is concordant with those of other cadaveric[2,6,8,11–15] and remnologic series[19] (Table 4). While this junction is usually lower in men than in women[15,19], we observed the converse (L1L2 disc in women, T12L1 disc in men). The median level of the iFT-DS junction corresponded to the lower third of S2, which is one-third vertebra lower than in the other studies[2,6,12,13,19] (Table 4) and did not vary according to the sex, contrary to what has been observed by Mac Donald *et al.*[19] These conflicting data could suggest that the level of the CM-iFT and iFT-DS-eFT junctions are gender independent. The eFT ended at the second coccygeal vertebra in 80% of cases, which confirms that its termination level is more stable than the levels of the CM-iFT and iFT-DS-eFT junctions.[2]

The level of the CM-iFT junction was correlated with the length of the iFT, which is consistent with the relatively low variability of the iFT-DS junction level. This correlation had already been demonstrated by Pinto et al[12] but is not consensual.[2] Besides, we do not confirm the significant correlation between the level of the iFT-DS junction and the length of the eFT[2], nor the correlation between the levels of the CM-iFT and the iFT-DS-eFT junctions.[12]

These discordant results could be related to statistical power and a larger sample may be required to conclude. Ethnical differences may also have contributed as not all previously published data were obtained in European specimens. Nevertheless, no correlation has been constantly found in the other studies. Subsequently, the clinical application of these results requires caution because of several biases including measurements after removal, in old specimens and overestimation of nervous structures in cadavers.[20]

The tractions performed during the dissections highlighted the damping role played by the FT, since its mobilization in one of its compartments (iFT or eFT) was not transmitted to the elements of the other compartment. Accordingly, Tubbs *et al.* noticed that the traction of the eFT induced no movement of the iFT[7]. The application of increasing loads demonstrated that the FT loses its elasticity more rapidly than the SC in animals and in humans, which confirms that the FT protects the SC against mechanical stress.[2,5,21,22] The identification of a multicellular structure, that may correspond to a mechanoreceptor, close to SMC in one specimen, could suggest that the eFT is able to self-regulate its tension. For some authors, the loss of FT elastic properties is linked to histological changes[23–26], results in a lowering of the CM-iFT junction (below L2 body[2,5]), and could lead to myelopathy development described as thethered cord syndrome.[5,9,12,27,28]

From embryology to histology and histopathology

During secondary neurulation, the FT originates from the SC located downstream of the 31st metameric segment.[1] Vacuolization and apoptotic phenomena[2,23,29] are responsible for the dedifferentiation of this structure that is redifferentiated into fibrous tissue.[1,4,5] Microscopic examination of human fetal SC reveals GC, ependymal and neuroblastic or neuronal cell bodies that are or not subjected to degenerative processes.[1,24,30] Subsequently, the adult FT is likely to contain the same tissue elements as the SC.[4,10] Furthermore, the recent identification of neuronal and glial stem cells in rat and human FT[31] confirms that this structure is far more complex than a simple ligament.

The performance of longitudinal sections is original. Neuronal bodies, axons that were sometimes myelinated and ependymocytes were identified within the iFT, as previously described[3,7,30,32] This could explain the development of ependymomas within the iFT[7].

Nevertheless, the decreasing frequency of these elements following a cranio-caudal gradient usually described [3,7,32], needs to be nuanced; even though the cell density is higher proximally, islands of ependymocytes are identifiable all along the iFT and are rather randomly distributed.

Consistent with the only description of the iFT-DS junction[2], we also observed that the outer fibrous layer of the DS blends almost imperceptibly into the fibrous stroma of the FT. Strikingly, we noted that the density of GC was particularly high at this level, that would explain the occurrence of gangliocytomas, paragangliomas[33,34] and ganglioneuroblastomas.[35]

Examination of the eFT found axonal structures, SMC, and adipose tissue. The absence of ependymal cells, as previously described[7], indicates that coccygeal ependymomas would more probably arise from subcutaneous coccygeal ependymal residues rather than from the eFT.[7] Contrary to Tubbs *et al.*, we did not find residues of meningothelial tissue or GC within the eFT.[7] The presence of adipose and meningothelial tissue within FT is sometimes considered as pathological.[24,36] This remark should consequently only apply to the iFT.

CONCLUSIONS

In accordance with their common embryological origin, there is a true anatomical and histological *continuum* between the CM and the FT. The biomechanical role played by the FT is particularly important and the identification of a mechanoreceptor, thanks to longitudinal sections, suggests potential self-regulatory mechanisms. Subsequently, this study definitively confirms that the FT should no longer be considered as a simple ligament but rather as a complex fibro-cellular structure.

Word count: 2993 words

Financial support: No funding was received for this research.

Conflict of interest: The authors declare that they have no conflict of interest.

Ethical approval: No ethics committee approval was required as the human cadavers were donated to the laboratory for anatomical and/or histological purposes.

REFERENCES

1. Streeter GL. Factors involved in the formation of the filum terminale. *Am J Anat*. 25(1):1-11. doi:10.1002/aja.1000250102

2. De Vloo P, Monea AG, Sciot R, van Loon J, Van Calenbergh F. The Filum Terminale: A Cadaver Study of Anatomy, Histology, and Elastic Properties. *World Neurosurg*. 2016;90:565-573.e1. doi:10.1016/j.wneu.2015.12.103

3. Jang HS, Cho KH, Chang H, Jin ZW, Rodriguez-Vazquez JF, Murakami G. The Filum Terminale Revisited: A Histological Study in Human Fetuses. *Pediatr Neurosurg*. 2016;51(1):9-19. doi:10.1159/000439284

4. Pearson AA, Sauter RW. Observations on the caudal end of the spinal cord. *Am J Anat*. 1971;131(4):463-469. doi:10.1002/aja.1001310406

5. Saker E, Henry BM, Tomaszewski KA, et al. The Human Central Canal of the Spinal Cord: A Comprehensive Review of its Anatomy, Embryology, Molecular Development, Variants, and Pathology. *Cureus*. 2016;8(12):e927. doi:10.7759/cureus.927

6. Hansasuta A, Tubbs RS, Oakes WJ. Filum terminale fusion and dural sac termination: study in 27 cadavers. *Pediatr Neurosurg*. 1999;30(4):176-179. doi:10.1159/000028790

7. Tubbs RS, Murphy RL, Kelly DR, Lott R, Salter EG, Oakes WJ. The filum terminale externum. *J Neurosurg Spine*. 2005;3(2):149-152. doi:10.3171/spi.2005.3.2.0149

8. Reimann AF, Anson BJ. Vertebral level of termination of the spinal cord with report of a case of sacral cord. *Anat Rec*. 88(1):127-138. doi:10.1002/ar.1090880108

9. Fontes RBV, Saad F, Soares MS, de Oliveira F, Pinto FCG, Liberti EA. Ultrastructural study of the filum terminale and its elastic fibers. *Neurosurgery*. 2006;58(5):978-984; discussion 978-984. doi:10.1227/01.NEU.0000210224.54816.40

10. Harmeier JW. The normal histology of the intradural filum terminale. *Arch Neurol Psychiatry*. 1933;29(2):308-316. doi:10.1001/archneurpsyc.1933.02240080098008

11. McCotter. Regarding the length and extent of the human medulla spinalis. *Anat Rec*. 1916;10. doi:10.1002/ar.1090100902

12. Pinto FCG, Fontes RB de V, Leonhardt M de C, Amodio DT, Porro FF, Machado J. Anatomic study of the filum terminale and its correlations with the tethered cord syndrome. *Neurosurgery*. 2002;51(3):725-729; discussion 729-30.

13. Trotter M. Variations of the sacral canal; their significance in the administration of caudal analgesia. *Curr Res Anesth Analg*. 1947;26(5):192-202.

14. Needles JH. The caudal level of termination of the spinal cord in american whites and american negroes. *Anat Rec*. 1935;63(4):417-424. doi:10.1002/ar.1090630409

15. Thomson A. Fifth Annual Report of the Committee of Collective Investigation of the Anatomical Society of Great Britain and Ireland for the Year 1893-94., Fifth Annual Report of the Committee of Collective Investigation of the Anatomical Society of Great Britain and Ireland for the Year 1893-94. *J Anat Physiol J Anat Physiol*. 1894;29, 29(Pt 1, Pt 1):35, 35-60.

16. Moore GE, Peyton WT. The clinical use of sodium fluorescein and radioactive diiodofluorescein in the localization of tumors of the central nervous system. *Minn Med*. 1948;31(10):1073-1076.

17. Nasr AY, Hussein AM, Zaghloul SA. Morphometric parameters and histological Study of the Filum Terminale of Adult human cadavers and MR images. *Folia Morphol*. May 2018. doi:10.5603/FM.a2018.0041

18. Benet A, Rincon-Torroella J, Lawton MT, González Sánchez JJ. Novel embalming solution for neurosurgical simulation in cadavers. *J Neurosurg*. 2014;120(5):1229-1237. doi:10.3171/2014.1.JNS131857

19. Macdonald A, Chatrath P, Spector T, Ellis H. Level of termination of the spinal cord and the dural sac: a magnetic resonance study. *Clin Anat N Y N*. 1999;12(3):149-152. doi:10.1002/(SICI)1098-2353(1999)12:3

20. Choi D, Carroll N, Abrahams P. Spinal cord diameters in cadaveric specimens and magnetic resonance scans, to assess embalming artefacts. *Surg Radiol Anat SRA*. 1996;18(2):133-135.

21. Tani S, Yamada S, Fuse T, Nakamura N. [Changes in lumbosacral canal length during flexion and extension--dynamic effect on the elongated spinal cord in the tethered spinal cord]. *No To Shinkei*. 1991;43(12):1121-1125.

22. Tani S, Yamada S, Knighton RS. Extensibility of the lumbar and sacral cord. Pathophysiology of the tethered spinal cord in cats. *J Neurosurg*. 1987;66(1):116-123. doi:10.3171/jns.1987.66.1.0116

23. Selçuki M, Vatansever S, Inan S, Erdemli E, Bağdatoğlu C, Polat A. Is a filum terminale with a normal appearance really normal? *Childs Nerv Syst ChNS Off J Int Soc Pediatr Neurosurg*. 2003;19(1):3-10. doi:10.1007/s00381-002-0665-1

24. Tehli O, Hodaj I, Kural C, Solmaz I, Onguru O, Izci Y. A comparative study of histopathological analysis of filum terminale in patients with tethered cord syndrome and in normal human fetuses. *Pediatr Neurosurg*. 2011;47(6):412-416. doi:10.1159/000338981

25. Liu F-Y, Li J-F, Guan X, Luo X-F, Wang Z-L, Dang Q-H. SEM study on filum terminale with tethered cord syndrome. *Childs Nerv Syst ChNS Off J Int Soc Pediatr Neurosurg*. 2011;27(12):2141-2144. doi:10.1007/s00381-011-1414-0

26. George TM, Bulsara KR, Cummings TJ. The immunohistochemical profile of the tethered filum terminale. *Pediatr Neurosurg*. 2003;39(5):227-233. doi:10.1159/000072866

27. Filippidis AS, Kalani MY, Theodore N, Rekate HL. Spinal cord traction, vascular compromise, hypoxia, and metabolic derangements in the pathophysiology of tethered cord syndrome. *Neurosurg Focus*. 2010;29(1):E9. doi:10.3171/2010.3.FOCUS1085

28. Yamada S, Won DJ, Pezeshkpour G, et al. Pathophysiology of tethered cord syndrome and similar complex disorders. *Neurosurg Focus*. 2007;23(2):E6. doi:10.3171/FOC-07/08/E6

29. Hertzler DA, DePowell JJ, Stevenson CB, Mangano FT. Tethered cord syndrome: a review of the literature from embryology to adult presentation. *Neurosurg Focus*. 2010;29(1):E1. doi:10.3171/2010.3.FOCUS1079

30. Gamble HJ. Electron microscope observations upon the conus medullaris and filum terminale of human fetuses. *J Anat*. 1971;110(Pt 2):173-179.

31. Chrenek R, Magnotti LM, Herrera GR, Jha RM, Cardozo DL. Characterization of the Filum terminale as a neural progenitor cell niche in both rats and humans. *J Comp Neurol*. 2017;525(3):661-675. doi:10.1002/cne.24094

32. Choudhary KK, Bhytani A, Agarwal R, Madan VS. Extradural myxopapillary ependymoma with sacral osteolysis--a case report. *Indian J Pathol Microbiol*. 2002;45(3):363-365.

33. Pytel P, Krausz T, Wollmann R, Utset MF. Ganglioneuromatous paraganglioma of the cauda equina--a pathological case study. *Hum Pathol*. 2005;36(4):444-446. doi:10.1016/j.humpath.2005.01.024

34. Shankar GM, Chen L, Kim AH, Ross GL, Folkerth RD, Friedlander RM. Composite ganglioneuroma-paraganglioma of the filum terminale. *J Neurosurg Spine*. 2010;12(6):709-713. doi:10.3171/2009.12.SPINE09482

35. Okudera Y, Miyakoshi N, Sugawara T, et al. Ganglioneuroblastoma of filum terminale: case report. *J Neurosurg Spine*. 2014;21(2):270-274. doi:10.3171/2014.4.SPINE121002

36. Pang D, Zovickian J, Wong S-T, Hou YJ, Moes GS. Limited dorsal myeloschisis: a not-so-rare form of primary neurulation defect. *Childs Nerv Syst ChNS Off J Int Soc Pediatr Neurosurg*. 2013;29(9):1459-1484. doi:10.1007/s00381-013-2189-2

FIGURE CAPTIONS

Fig. 1 *Anatomical study of the different portions of the Filum Terminale.*

The orientation is the same for all pictures (left = cranial, right = caudal). Pictures were taken with a digital camera (A - x4 magnification) or a surgical microscope (B and C - x40 magnification) (D and E – x10 magnification).

The very cranial portion of the iFT is anterior to the lumbar and sacro-coccygeal roots and is subsequently not visible immediately after opening the dura mater (A). The interface between the CM and the iFT corresponds to a progressive transition zone marked by a progressive disappearance of the nervous tissue that is replaced by fibrous tissue organized in linear spans (B). The space delimited by black arrows highlights the continuum between the iFT and the DS. The term "fusion" seems appropriate to describe the FT-DS junction, both in the intra-dural and extra-dural spaces (C). Example of eFT caudal periosteal insertion with a single bundle marked with a black arrow (D). Example of eFT caudal periosteal insertion with several bundles, marked with black arrows, that were fan-shaped (E).

CM = Conus Medullaris, DS = Dural Sac, eFT = extradural Filum Terminale, iFT = intradural Filum Terminale

Fig. 2 *Representation of vertebral projections of:*

- *the Conus Medullaris – intradural Filum Terminale junction (*),*
- *the Filum Terminale – Dural Sac junction (#), and*
- *the extradural Filum Terminale - coccyx junction (-).*

Fig. 3 *Schematic representation of the Filum Terminale with pictures corresponding to the different levels (x400).*

The CM-iFT junction contains small rootlets included in the iFT stroma (A), ependymal cells organized as a rosette (B) and ganglion cells randomly distributed at the CM-iFT junction (C) which display positive immunostaining for NeuN (insert).

The First half of the iFT contains isolated ganglion cells (D) and amyloid bodies which are frequently found in cellular areas (E). Nervous rootlets are directly contiguous to the iFT (F).

The second half of the iFT is also contiguous to myelinated rootlet, as highlighted by luxol-fast-blue coloration (G). Groups of axons are included in the iFT (H), as attested by the immunopositivity for neurofilament (I).

In the FT-DS junction, the density of ganglion cells is particularly high (J).

<u>In the first half of the eFT</u>, a structure composed of a circular cluster of neuronal cells organized in sheets was found and probably corresponded to a mechanoreceptor (K). Group of axons are surrounded by linear groups of smooth muscle cells (L). Calcospherites (one of which is partially broken) are found in connective tissue (M).

<u>The Second half of the eFT</u> contains smooth muscle cells (N), as attested by the positive immunostaining for actin (insert). A huge amount of adipose cells is found around the distal eFT. Adipose cells are also present within the eFT (O). Winding-up of fibrous tissue are observed (P).

CM = Conus Medullaris, DS = Dural Sac, eFT = extradural Filum Terminale, iFT = intradural Filum Terminale

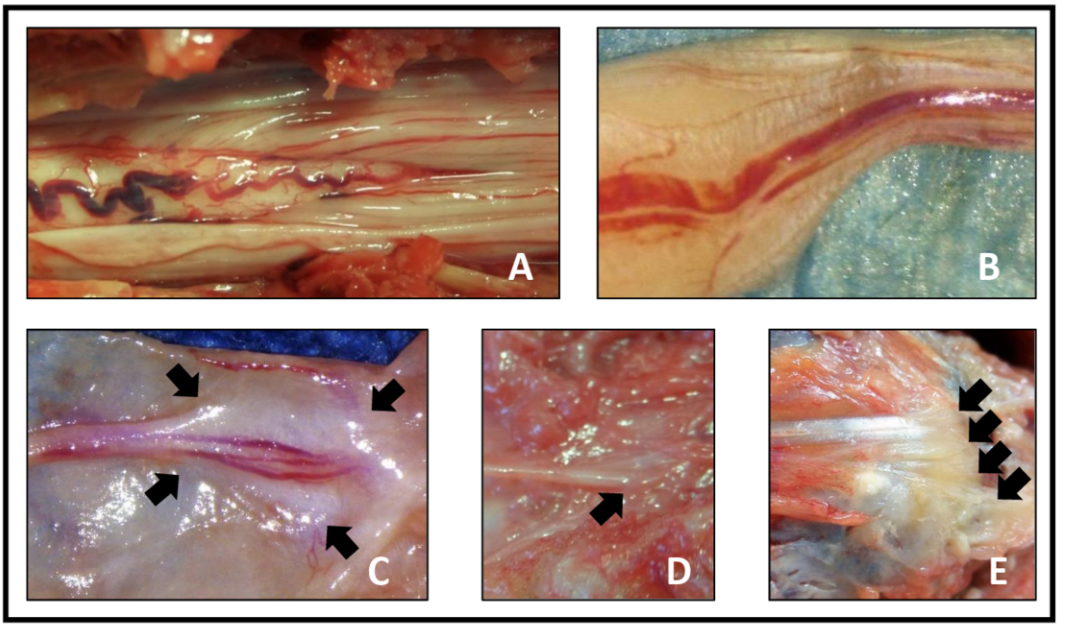
A
B
C
D
E

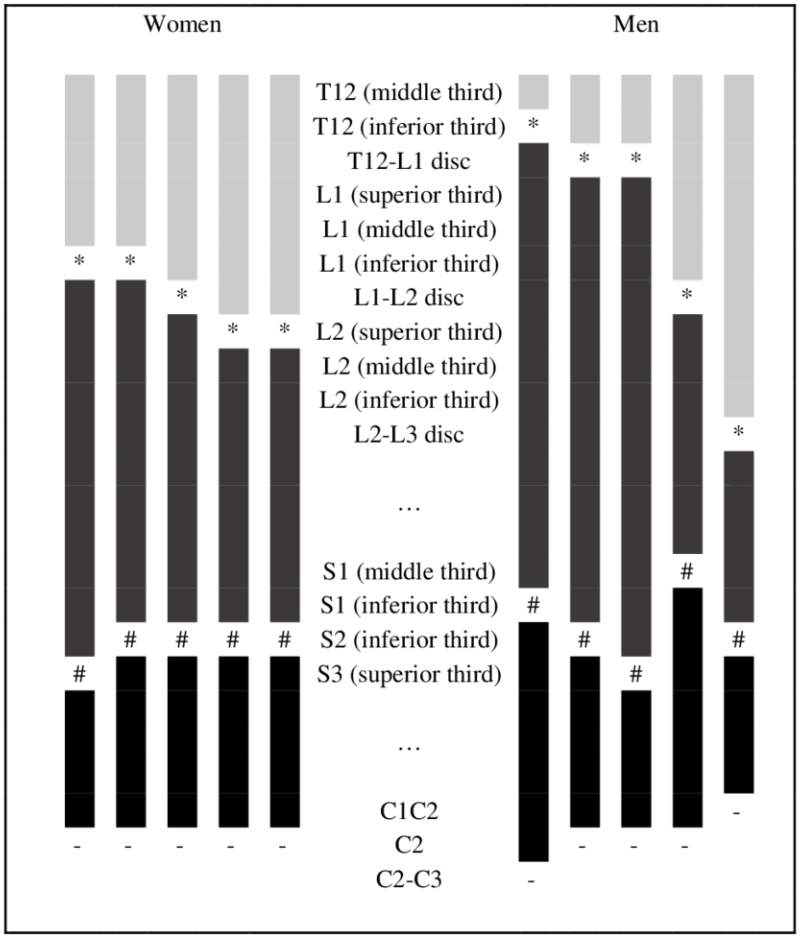
Women
Men
T12 (middle third)
T12 (inferior third)
T12-L1 disc
L1 (superior third)
L1 (middle third)
L1 (inferior third)
L1-L2 disc
L2 (superior third)
L2 (middle third)
L2 (inferior third)
L2-L3 disc
…
S1 (middle third)
S1 (inferior third)
S2 (inferior third)
S3 (superior third)
…
C1C2
C2
C2-C3

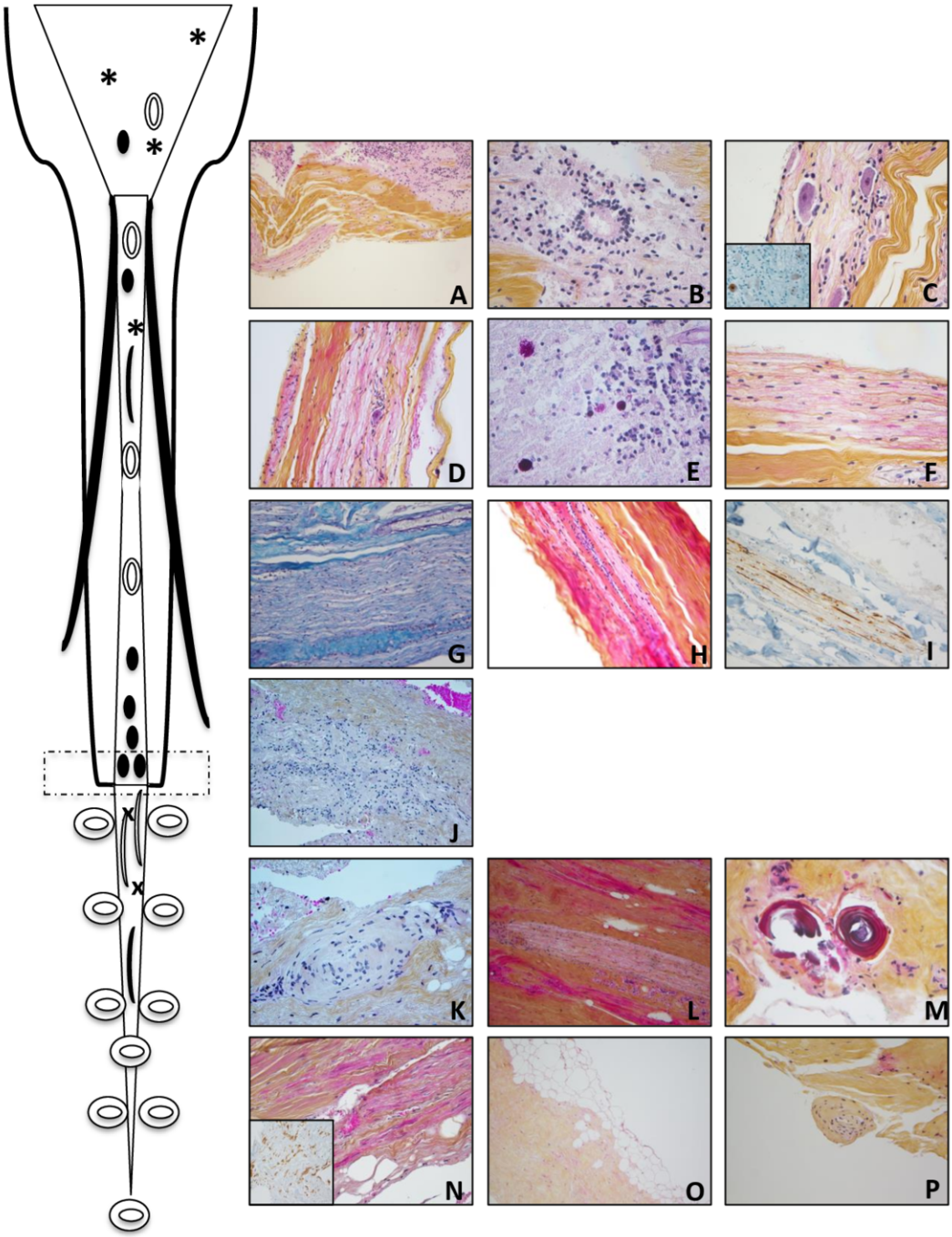

Legend:

- Ependymocyte
- Ganglion cell
- Adipose cell
- Smooth muscle cell
- Axon (partially represented)
- x Calcospherite
- * Amyloid body

	Mean	Minimum	Maximum
Age (years)	85.2	59	96
Height (cm)	160.2	145	175
Weight (kg)	58.1	40	83
Body Mass Index (kg/m^2)	22.4	18.8	27.1
Time since death (days)	19.4	10	32

Table 1: Demographic characteristics of the specimens

	Mean	SD	Minimum	Maximum
iFT length (mm)	167.13	21.69	135	190
Cranial iFT diameter (mm)	1.84	0.34	1.40	2.57
First quarter iFT diameter (mm)	0.88	0.20	0.56	1.16
Half iFT diameter (mm)	0.71	0.22	0.44	1.14
Third quarter iFT diameter (mm)	0.67	0.30	0.30	1.38
Caudal iFT diameter (mm)	0.74	0.24	0.44	1.12
eFT length (mm)	87.59	17.46	71.11	127
Cranial eFT diameter (mm)	1.05	0.38	0.48	1.72
Half eFT diameter (mm)	0.77	0.22	0.42	1.15
Caudal eFT diameter (mm)	0.59	0.24	0.36	1.02

Table 2: Morphometric parameters of the different segments of the intradural Filum Terminale and extradural Filum Terminale in the present series (expressed in millimeters)

eFT = extradural Filum Terminale, iFT = intradural Filum Terminale, SD = Standard Deviation

	Number of specimens	Mean length	Cranial diameter	1st quarter diameter	Half diameter	3rd quarter diameter	Termination diameter
iFT							
Pinto *et al*, 2002[12]	41	156.44	1.38		0.76		
Fontes *et al*, 2006[9]	20	155.4	1.56		1.03		
De Vloo *et al*, 2016[2]	20	158.75	1.93	0.99	0.85	0.71	0.69
Nasr *et al*, 2018[17]	25	162.3	1.7		0.74		
Present series	**10**	**167.14**	**1.84**	**0.87**	**0.71**	**0.68**	**0.74**
eFT							
Harmeier, 1933[10]	Not specified	+/- 80					
Tubbs *et al*, 2005[7]	15	+/- 80			+/- 1		
De Vloo *et al*, 2016[2]	20	69.33	1.07		0.75		1.03
Nasr *et al*, 2018[17]	25	74.8			0.48		
Present series	**10**	**87.59**	**1.05**		**0.77**		**0.59**

Table 3: Comparison of the length and diameter of the intradural Filum Terminale and extradural Filum Terminale (expressed in millimetres), according to other published series[2, 7, 9, 10, 12, 17]

eFT = extradural Filum Terminale, iFT = intradural Filum Terminale

	Type of study	Number of specimens	Median level of CM-iFT junction	Range of CM-iFT junction	Median level of FT-DS junction
Thomson, 1894[15]	Unspecified	198	Inferior third of L1	Middle third of T12 Superior third of L3	
Mc Cotter, 1916[11]	Unspecified	234	Inferior third of L1	Inferior third of T12 Superior third of L3	
Needles, 1935[14]	Unspecified	240	Superior third of L2	Middle third of T12 Inferior third of L3	
Reimann, Anson, 1944[8]	Unspecified	129	L1-L2 disc	Inferior third of T12 Middle third of L3	
Trotter, 1947[13]	Bone	1227			Middle of S2
Hansasuta *et al*, 1999[6]	Unspecified	27			Middle of S2
Mac Donald *et al*, 1999[19]	MRI	136	Middle third of L1	Middle third of T11 Middle third of L3	Middle third of S2
Pinto *et al*, 2002[12]	Cadaveric (fresh)	41	Middle of L1		Superior part of S2
De Vloo *et al*, 2016[2]	Cadaveric (fresh and embalmed)	20	Inferior third of L1	Middle third of T12 Superior third of L3	Middle of S2
Present series	**Cadavers (fresh)**	**10**	**Inferior third of L1 and L1L2 disc**	**Inferior third of T12 L2L3 disc**	**Inferior third of S2**

Table 4: Comparison of the levels of Conus Medullaris -intradural Filum Terminale and Filum Terminale-Dural Sac junctions according to other published cadaveric and MRI series[2, 6, 8, 11, 12, 13, 14, 15, 19]

CM = Conus Medullaris, iFT = intradural Filum Terminale, DS = Dural Sac